Hydrological Processes

WILEY

RESEARCH ARTICLE OPEN ACCESS

Assessing Mountain Soil Water Storage and Release in a Colombian Páramo With APSIS-InSAR Data

Andrew V. Bradley[1] | David J. Large[2] | Jeffrey Mauricio Prieto Naranjo[3] | Wouter Buytaert[4] | Emily Mitchell[5] | Andrew Sowter[6] | Mauricio Diazgranados[7,8] | Boris Ochoa-Tocachi[4,9] | Charles George[10] | France F. Gerard[10]

[1]University of Nottingham, Nottingham Geospatial Institute, Nottingham, UK | [2]Department of Chemical and Environmental Engineering, Faculty of Engineering, University of Nottingham, Nottingham, UK | [3]Hydrology and Ecosystem Modeling, National University of Colombia, Medellín, Colombia | [4]Faculty of Engineering, Department of Civil and Environmental Engineering, Imperial College London, London, UK | [5]School of Mathematical Sciences, University of Nottingham, Nottingham, UK | [6]Terra Motion Limited, Ingenuity Centre, Innovation Park, Jubilee Campus, University of Nottingham, Nottingham, UK | [7]New York Botanical Garden, New York, New York, USA | [8]Royal Botanic Gardens, Kew, Richmond, UK | [9]ATUK Consultoría Estratégica, Cuenca, Ecuador | [10]UK Centre for Ecology & Hydrology, Oxfordshire, UK

Correspondence: Andrew V. Bradley (andrew.bradley1@nottingham.ac.uk)

Received: 9 October 2024 | **Revised:** 22 May 2025 | **Accepted:** 9 July 2025

Funding: This work was supported by the Natural Environment Research Council, United Kingdom, project PARAGUAS, grant NE/R017654/1.

Keywords: bofedal | catchment storage | flow paths | ISBAS | satellite radar | tropical Andes

ABSTRACT

Direct observation of montane and upland water resources provides valuable data in support of national scale water management and policy, but direct observation is challenging on large spatial scales. To address the need for large spatial scale hydrological data we use InSAR surface motion signals, indicative of surface swelling due to increased soil water content, at approximately 90 m resolution over a tropical Colombian mountain range covered with Páramo, a biome widespread along the Northern Andes. Considering uncertainty of vegetation and mountainous terrain on the InSAR signal, we observe a regional, spatially consistent sequence of soil surface motion, which can be related to storage and movement of water through montane catchments. Swelling on the ridges and upper slopes occurs during the wet season and is consistent with infiltration and increased saturation of ridge and upper slope soils. This is followed by a marked swelling of the valley floors towards the end of the wet season and into the dry season. The InSAR signal also captures movement of water through the basin with swelling subsiding sequentially downslope and downstream. The results indicate that a shallow hillslope flow dominates during the wet season, but this alone is insufficient to explain shallow ground water storage in superficial valley deposits lasting into the late wet season and dry season. We conclude that InSAR signals can provide a qualitative insight in the storage and release mechanisms at a basin scale, thus complementing sparse point-scale measurements.

1 | Introduction

The tropical Andes in South America comprise montane and upland environments that play a crucial role in the capture and storage of freshwater that supports agriculture, human population (Buytaert et al. 2006; Roa-García et al. 2011), endemic species, biodiversity (Squeo et al. 2006) and carbon storage (Comas et al. 2017). Climate change will have impacts on the hydrology of these montane environments (Aggarwal et al. 2022; Bradley et al. 2006; Mills-Novoa et al. 2017) and representative data is crucial in supporting the models on which policy decisions are based (Sidle 2021). However, the understanding of Andean hydrological systems is much more limited compared to other mountain regions of the world (Brück et al. 2023; Mosquera et al. 2023) and needs to be at an appropriate spatial scale to cover the diversity of hydrological processes (Somers and McKenzie 2020). In turn, this will enable governments to justify, develop, and implement policies to improve management of upland catchments and their associated dependencies. Problematically, direct observations are limited by high experimental costs, poor access to remote locations, and the social and political pressures that make field work challenging (Somers and McKenzie 2020; Sheffield et al. 2018). As a result, detailed hydrological measures tend to be small scale and highly localised, making it hard to validate regional models of any type at an appropriate scale (Sheffield et al. 2018).

To help address this need for low-cost, multiscale, hydrological evidence we present a new means of visualising montane basin hydrology in the high-altitude soils, which we apply to a case study in the Páramo of Colombia, an Andean biome that generally occurs between 2800 and 4700 m a.s.l. (Giles et al. 2017). We use interferometric synthetic aperture radar (InSAR) to quantify swelling and shrinking of soils in response to changes in water storage. InSAR has previously shown shrinking and swelling in valley bottom sediments due to poroelasticity (Kang and Knight 2023) and hydraulic head (Smith et al. 2017; Smith and Knight 2019) at kilometre scales. This method has the potential to show spatio-temporal changes in soil water storage at a resolution of 10s of metres within basins on scales ranging from 10s to > 100s km and improve gaps in our understanding of the processes that influence water capture, storage, and flow within montane systems. The main influences are: groundwater (Somers and McKenzie 2020), soils (Correa et al. 2017), vegetation (Bounous et al. 2018)—including bofedal (Maldonado Fonkén 2014; Earle et al. 2003; Moreau et al. 2003; Valois et al. 2020) grasslands, shrublands, and *Espeletia* spp. (Cárdenas et al. 2018) that are found in páramo—complex geology (Cetina et al. 2020; Valois et al. 2020), agricultural activities (Moreau et al. 2003; Valois et al. 2020), and land cover change (Crespo et al. 2009; Ochoa-Tocachi et al. 2016).

Our method uses freely available regular 12-day ESA Sentinel-1 SAR data acquisitions that can penetrate cloud. In conjunction with improved InSAR (Interferometric SAtellite Radar) methods (Cigna and Sowter 2017; Sowter et al. 2013; Sowter et al. 2016) these data can generate time series of land surface deformation with near-continuous spatial coverage. The method has been developed and used for assessment of peat soils (Alshammari et al. 2020; Bradley et al. 2022; Islam et al. 2022; Large et al. 2025; Mitchell et al. 2025). In these applications, signals derived from the time series of surface motion are used to classify the physical and ecohydrological state of the peatland (Bradley et al. 2022), condition (Large et al. 2025) and trajectory of change (Mitchell et al. 2025). The approach has been validated against simultaneous field observations (Marshall et al. 2022) and works because the InSAR surface motion signal responds to changes in water storage within the soil (Tampuu et al. 2020; Toca et al. 2022; Hrysiewicz et al. 2023), which in turn is regulated by the ecohydrological dynamics of the system (Alshammari et al. 2020; Bradley et al. 2022). An important point is that the method uses a signal that precisely represents differences in the motion of the soil surface with time, but it underestimates the true magnitude of surface motion (Marshall et al. 2022), providing a consistent qualitative measure which must not be treated as an accurate measure.

Application of this method to the páramo carries with it several uncertainties. Páramo soils are not predominantly peat soils and the associated plant species are very different to those of temperate peatlands. So, although shrinking and swelling may be expected in response to changing water storage, the range of motion will likely be less than peat and governed by different soil properties and ecohydrology. Precipitation seasonality is very different to that encountered in the temperate peat soils in northern Europe, which will impact the observed pattern of changes. Associated with the seasonality and difference in soil is the uncertainty as to whether the SAR signal scatters from the soil surface detecting true motion or at a depth within the soil where moisture levels stop further radar penetration. Whilst increased penetration is obvious over bare ground when volumetric soil moisture levels become very low, soil moisture effects are masked in the presence of vegetation, leading to some debate over whether sub-centimetre surface movement can be soil moisture change or seasonal vegetation growth (Westerhoff and Steyn-Ross 2020). With a permanent presence of thick grass or shrubby páramo vegetation preventing the subsurface from drying out, we consider the impact of soil moisture variation to be minor. With this in mind, any contribution from soil moisture variation is likely to drive soil swelling and that will not affect a qualitative analysis of surface motion. Whether the signal is responding to surface motion related to water content, a change in soil moisture, or both (Toca et al. 2022; Hrysiewicz et al. 2023), it should be possible to obtain data to describe water storage patterns.

If swelling of the soil corresponds to water storage, a large direct swelling in response to precipitation would indicate rapid infiltration and a relatively large water storage capacity, while little swelling in response to precipitation would indicate a reduced water storage capacity. A marked delay between precipitation and swelling could suggest that the water storage is influenced by lateral flow, storage in superficial deposits, or by shallow sub-surface flows and groundwater. So, if variable storage and lateral flow are occurring, we should see systematic patterns across the landscape, rather than highly varied noisy patterns which are difficult to interpret.

Our aim is to test the hypothesis that the spatial patterns of surface motion measured using the APSIS InSAR method are indicative of patterns of water storage and flow within the Páramo. To do this, we identify and map the spatial patterns of surface motion and qualitatively interpret them relative to the timing of precipitation in the wet and dry seasons. We then consider the potential implications of the observed relationships for understanding and quantifying the hydrological behaviour of Páramo environments.

2 | Study Area

2.1 | Páramo Guantiva-La Rusia

The study focuses on part of the Colombian Páramo known as Guantiva-La Rusia, Guantiva being the northern part of this páramo complex and La Rusia making up the southern part, with the analysis being contained to an area within approximately 40 × 60 km (Figure 1). The páramo is on a NE–SW

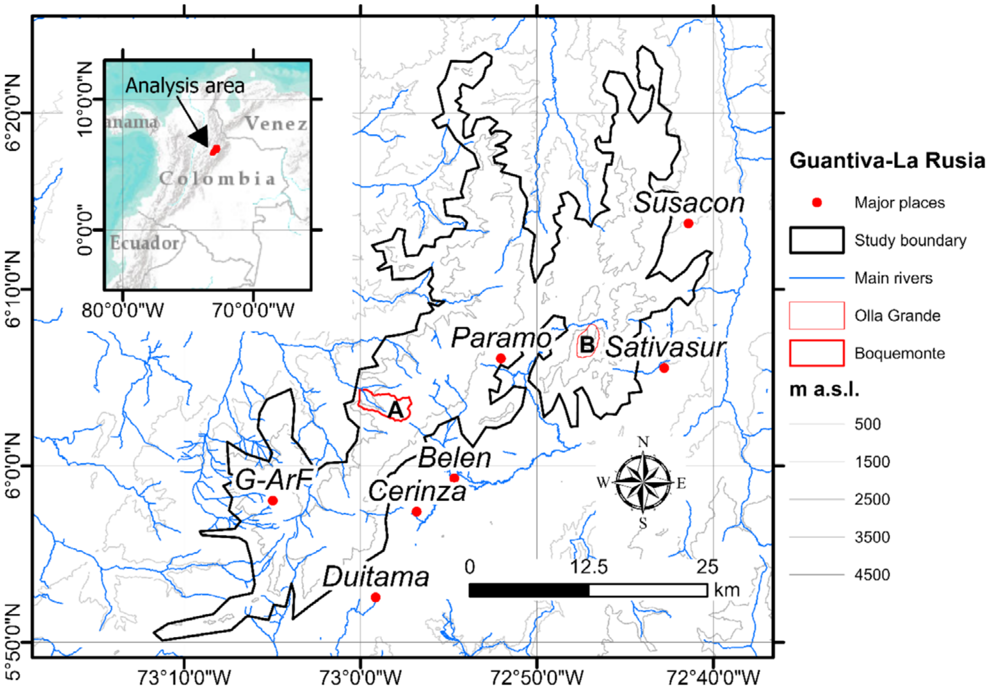

FIGURE 1 | Location of the basins used in this study, Boquemonte (A) and Olla Grande (B), within the Páramo of Guantiva-La Rusia. Also shown are the main settlements, the weather station G-ArF (Guanentá Alto Río Fonce—Parques Nacionales Naturales de Colombia) and the boundary of analysis. Contours derived from the SRTM DEM (Farr et al. 2007; Jarvis et al. 2008) and rivers sourced from (Schneider 2024).

trending western ridge approximately 55 km in length, rising from 2800 m a.s.l. to just over 4200 m a.s.l., straddling the border of the departments Santander and Boyacá, and a more northerly N-S trending eastern ridge in Boyacá approximately half as long, rising to 3800 m a.s.l. (Figure 1). The two ridges are linked by a lower plateau in the north, and from this watershed, three main valleys drain roughly north, northeast, and southwest from approximately 3200–3400 m a.s.l. Drainage on the outer sides of the ridges is generally northeast and northwest. Since it is difficult to define a páramo limit on altitude alone, we defined the boundaries of analysis to include the transition into the páramo environment, from just below the upper tree line, identified from ESRI world view images in ArcMap (ESRI 2024), into the predominantly short vegetation and agriculture above. When no tree line was observed, due to agricultural encroachment, the study boundary was determined by using roughly similar altitudes between 3000 and 3200 m a.s.l., guided by contours derived from the SRTM DEM (Farr et al. 2007; Jarvis et al. 2008).

For the purposes of this study, we perform InSAR analysis on the entire study area and focus in detail on two drainage basins with an elongated bowl-shaped morphology that represent the extremes of topographical geometries more or less replicated across this páramo. They also demonstrate if their slope orientation, almost parallel and perpendicular to the satellite line-of-sight, will cause any bias in the results. The two basins are Olla Grande (est. 6.2 km^2) and Boquemonte (est. 9.9 km^2). Olla Grande drains north and is a narrow, steep-sided valley with a flatter area in the upper middle reach and 2 hanging valleys (Figure 2), in the drier northeastern side of the páramo. Boquemonte is a west-draining basin on the wetter western edge of the páramo that is more open in the upper reaches of its northern side and steep and shrubby on its southern side (Figure 2). The upper reaches of Boquemonte contain 3 main hanging valleys, some containing several small, 10–100 m diameter pools. The ridge crests around Boquemonte are predominantly broad and grassy, whereas those around Olla Grande are narrower (Figure 2) with a mixture of vegetation and rock outcrops.

Geologically, the area is complex but generally consists of metamorphic rocks overlain by a mixture of superficial Quaternary deposits: glacial till, fluvio-glacial, fluvial, and solifluction deposits, and peat (Figure 3). Soils are mainly andosols, inceptosols, and histosols (IGAC 2005).

The vegetation at the top of the ridges is described as 'páramo', and contains a grass-shrub vegetation, endemic rosettes ('frailejones') and occasional boggy areas known as 'bofedal'. These grasslands transition into remnant montane forest on the steeper slopes, or suddenly into cultivated agricultural land, such as potato fields. In the flatter main valleys, vegetation is dominated by agriculture, and upper slopes and ridges have been used historically as rough pasture including the use of fire for management. The denser the biomass of these land covers, e.g., forest > shrubby > grasslands and pasture, and harvesting of crops in areas of cultivation will add noise and increase uncertainty to the surface motion calculation.

2.2 | Climate

The area experiences a bimodal precipitation regime with a distinct dry season that can fall between late November and late January, with another brief dry period around July. The major wet season falls between late January and July, followed by a wet period between late July and November (Robledo and

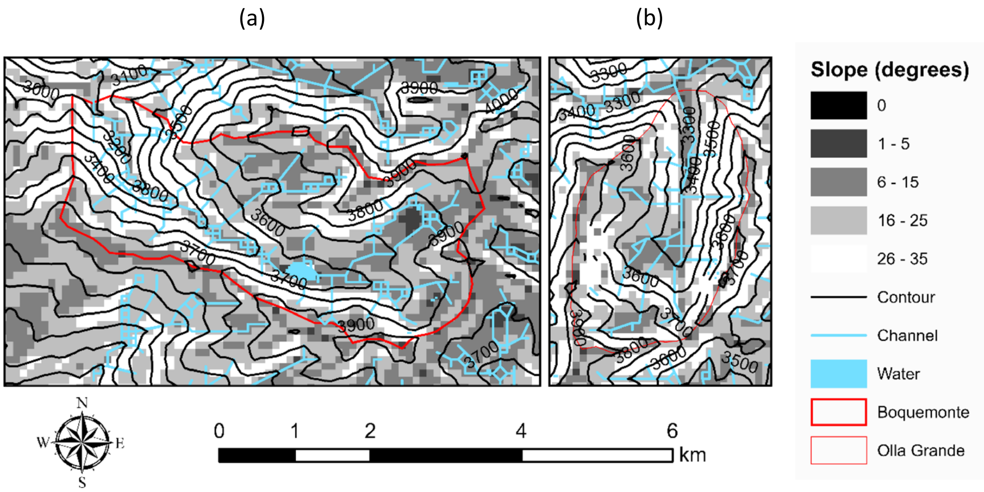

FIGURE 2 | Physical detail of (a) Boquemonte and (b) Olla Grande showing altitude, potential surface drainage, water bodies (Peyre et al. 2021) and slope angle calculated from the SRTM DEM (Farr et al. 2007; Jarvis et al. 2008).

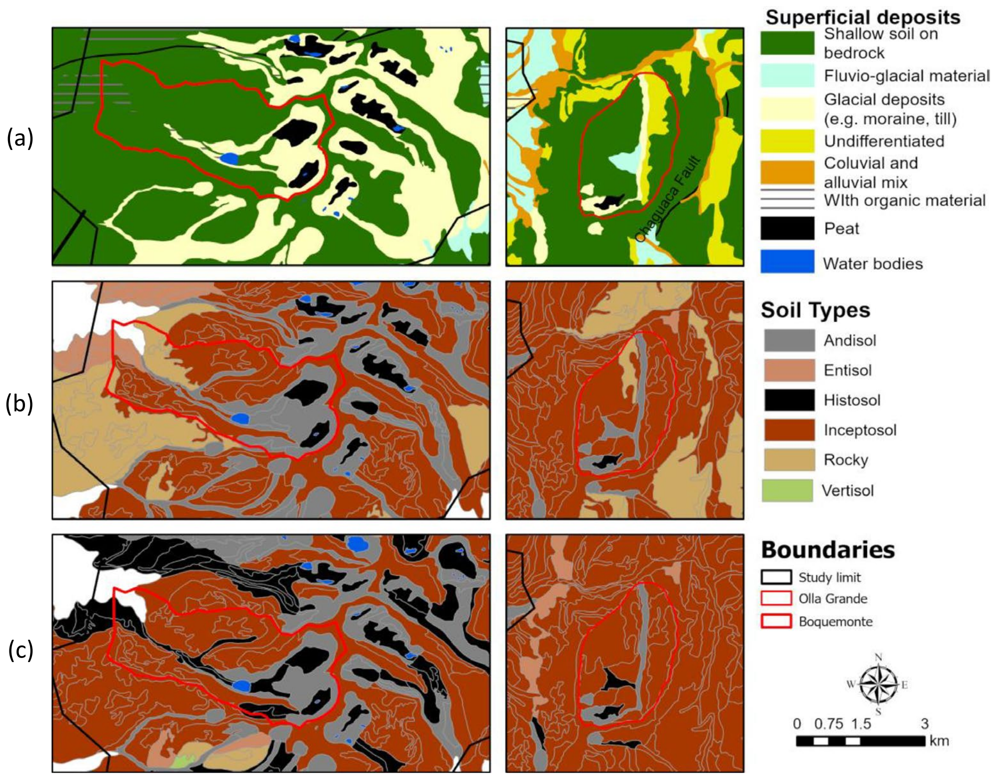

FIGURE 3 | Superficial material and soil deposits around Boquemonte (left) and Olla Grande (right). (a) Quaternary drift deposits. (b) Dominant and (c) sub dominant soil within soil units IGAC (2005).

Córdoba 2000; Cetina et al. 2020). Precipitation in the January to July wet season is generally greater. A weather station at UPTC in Tunja provides the nearest available detailed continuous meteorological data (IDEAM 2022) and this reflects the expected pattern of seasonal precipitation (Figure 4). Maximum daytime temperatures are generally around 25°C in the dry season, falling to 15°C in the wet season. To the best of our knowledge, the only reliable weather data collected within páramo Guantiva-La Rusia is from the hill station in the upper reaches of the protected area Santuario de Flora y Fauna Guanentá Alto Río Fonce (3760 m a.s.l, 5°58′8″ N, 73°5′7″ W). This area is considered wetter than Tunja, but the general precipitation trends are similar (Figure 4). For convenience, data from this source is referred to as data from Guanentá. We follow meteorological convention, presenting two full years from January, which is normally the driest part of the year and theoretically should contain a complete cycle of soil water storage and release. In the year 2017 (Figure 4a), precipitation data from Tunja indicates a relatively dry year. The main dry season was prolonged into February (~40 mm) and the major wet season rains (~> 100 mm) were not sustained through the smaller wet season after June, dropping to

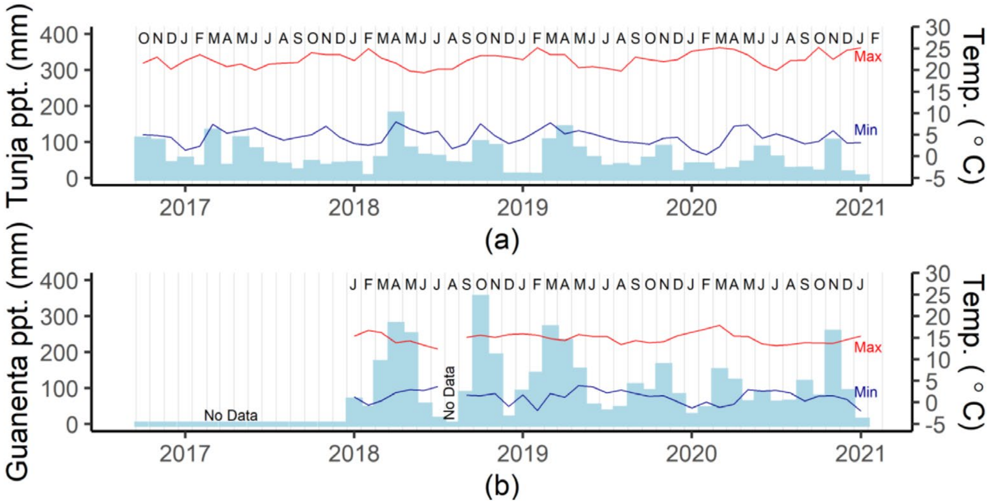

FIGURE 4 | Monthly precipitation and temperature measured at (a) Tunja (5°32′ 20″ N, 73°20′ 46″ W) 01 October 2016 to 31 January 2021 and (b) Guanentá Alto Río Fonce (5°58′8″ N, 73°20′ 46″ W) 01 January 2017 to 31 January 2021 (no data August 2018).

dry season equivalents for the remainder of the year (~40 mm). In comparison, it was much wetter at the end of the 2016 wet season (~100 mm). For the year 2019, data from Guanentá (Figure 4b) has two characteristic pulses of precipitation reflecting the strong bimodal wet season. The dry season ended early in December 2018 precipitation (16 mm) and the major wet season followed with a slightly early peak in March and April (~250 mm), declining into the short dry period by August (~35 mm). The smaller wet season peak followed this in November (~162 mm), before declining into the main dry period in the following January.

3 | Data and Methods

3.1 | Sentinel-1 Satellite Data and Processing

C-band satellite radar imagesfrom Sentinel-1A and-1B, 1B acquired every 12 days when possible (descending passes only) between March 2015 and October 2020. Data processing used the APSIS method (Sowter et al. 2013, 2016) which, to ensure independent coherence measures, resamples and reduces the original 20 by 5 m Sentinel-1 spatial resolution by a factor of 5 and 10 (called multi-looking) and creates a surface motion time series in the units of metres (m) for each multi-looked pixel. The APSIS algorithm guarantees that the InSAR measurements come from highly coherent areas, which provides confidence that we are seeing swelling as opposed to a change in vegetation cover or backscattering characteristics. As a check, multiannual velocity standard error, inversely proportional to the square root of coherence interferograms, shows the level of uncertainty of the ground motion (Cigna and Sowter 2017). For data management, we allowed spatial interpolation over areas of radar shadow, flagged as areas of high uncertainty. After orthographic correction from the multi-looked coordinate grid at roughly 80 by 90 m area, an irregularly spaced grid of points is produced, typically showing millimetre (mm) scale change between time points. Orthographic correction of radar data causes the point spacing to be generally closer on slopes facing the satellite sensor line-of-sight and wider apart on slopes facing away from the satellite sensor line-of-sight. Since raster interpolation would be forced to simulate data in the larger gaps and subsample closely spaced data, Thiessen polygons were calculated around each grid point, creating a continuous surface of polygons. For ease, in the rest of this article, we refer to each Thiessen polygon as a pixel. We do not correct for differences in pixel spatial area as the objectives are to understand broad patterns and trends rather than attempt to quantitatively calculate any hydrological budgets. We selected two periods for analysis, avoiding gaps in the data archive: 18 October 2016 to 26 June 2018 and 26 August 2018 to 03 October 2020. These two periods contain the dry seasons in 2016–17, 2017–18, 2018–19 and 2019–2020, the complete wet seasons in 2017, 2019 and the earlier part of the wet season in 2020.

3.2 | Detrending and Smoothing With Splines

Surface motion time series from APSIS InSAR reliably show annual cycles of motion, systematic trends controlled by climate (Bradley et al. 2022; Large et al. 2025) and short-term responses to drought or precipitation (Islam et al. 2022; Mitchell et al. 2025) with some level of noise superimposed. To isolate the underlying patterns in surface motion from any systematic linear trends and noise, a natural cubic spline (Mitchell et al. 2024) was fitted to each of the two sections of the time series to provide detrended smooth time series (Figure 5).

3.3 | Analysis of Surface Motion Relative to Patterns of Precipitation

Monthly relative surface motion displacement was calculated to compare each detrended and smoothed time series to precipitation and topographic setting. For each time series, the minimum value (Figure 5) was subtracted, and data was averaged into monthly intervals ($n = 3$). Monthly maps of surface motion for all points within Olla Grande and Boquemonte spanning the period of analysis were created to investigate

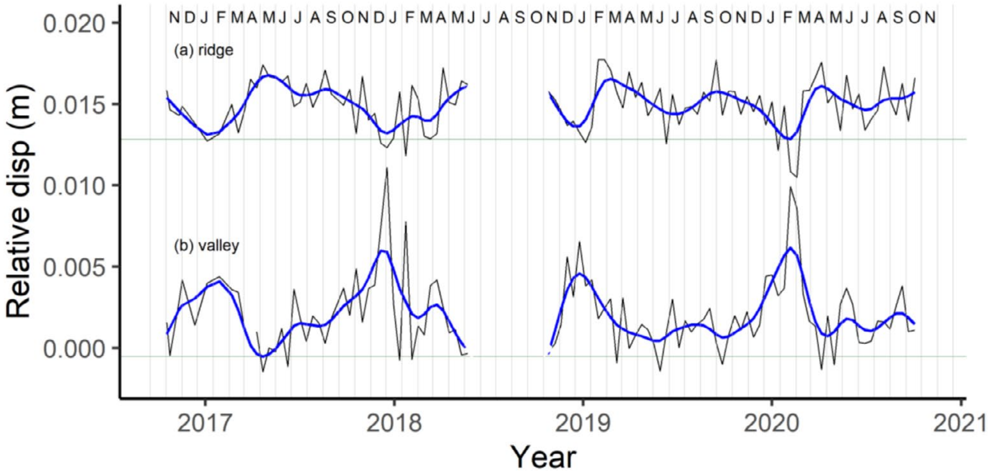

FIGURE 5 | Detrended and spline smoothed function of surface motion illustrating the timing of water capture, storage and release for the most generic scenarios on, (a) ridge tops and (b) valley floors (separated for visualisation by +0.009 m and +0.003 m respectively). The black line is the linearly detrended time series, blue is the resulting spline smoothed function. Amplitudes of peaks are determined relative to the horizontal line marking the minimum value of both time series.

the spatial and temporal pattern of the surface motion trends (Figures 6 and 7).

4 | Results

4.1 | Surface Motion Observations

In two full years, 2017 and 2019, surface motion in Olla Grande and Boquemonte indicated that surface swelling varied month by month, between ridges, slopes, and valleys, and was common across the rest of Guantiva-La Rusia. Overall, a repetitive cycle of surface swelling was observed, although the timing and length of the cycle varied inter-annually from the hypothesised January start. The variations in swelling, described below, bear a relationship to the amount of precipitation.

4.1.1 | Olla Grande

Much of the 2017 swelling on the ridges and slopes of Olla Grande (Figure 6) was in step with the observed precipitation (Figure 4). In the main dry season that prolonged into February, the ridges and slopes had low to very low swelling. When precipitation increased into June in the major wet season, the ridges experienced increased swelling to low and medium levels. Despite the lack of precipitation that followed in the smaller wet season, ridge swelling was sustained through July, areas of medium swelling then contracted, leaving greater areas of very low level swelling by October. Some westerly facing slopes retained greater local swelling before levels gradually fell to low and very low levels. By November and December, when precipitation had remained low, most of the ridges and slopes were at very low levels of swelling again. In contrast, valley swelling was often out of step with precipitation. During the dry season when precipitation was low, valley swelling had developed during January into localised patches of medium to high swelling. By April, as precipitation levels were increasing in the major wet season, these areas then contracted to be replaced by low and very low levels of swelling. From May to October 2017 in the second wet season, precipitation was lower than expected and medium levels of valley swelling gradually coalesced and extended back up and down the whole valley floor again. By November and December, with reduced precipitation, the valley featured high and very high levels of swelling over a much larger area of the valley floor. The full data sequence from October 2016 to May 2018 (SM Figure S1) illustrates that inter-annual timing of swelling varies outside the hypothesised January to December window.

As in 2017, although with less magnitude, most of the 2019 swelling on the ridges and slopes of Olla Grande (Figure 7) was again in step with precipitation and out of step with swelling in the valley. On the ridges, very low swelling during January developed into substantial patches of low to medium swelling during February and March as precipitation increased through the major wet season. This ridge swelling then contracted and almost vanished into very low swelling levels by August, as the major wet season weakened. A similar ridge swelling cycle repeated through September to December during the smaller wet season. In 2017, some eastern-facing slopes and southwest valley area stood out as having very low levels of swelling in the first cycle, which increased to low levels in the second cycle. In contrast, along the valley bottom, as the precipitation increased during the major wet season from January to March, swelling went from high to low with the exception of a localised patch in the north end of the valley. From April to September, when precipitation levels decreased, the swelling of a central core area increased to medium levels and spread back upstream and downstream in the valley. The swelling again became more localised during the peak of the second wet season during November. By December, as precipitation amount fell, accordingly swelling spread back along the valley again. The following dry season in January and February 2020 (SM Figure S2) then developed a dominant

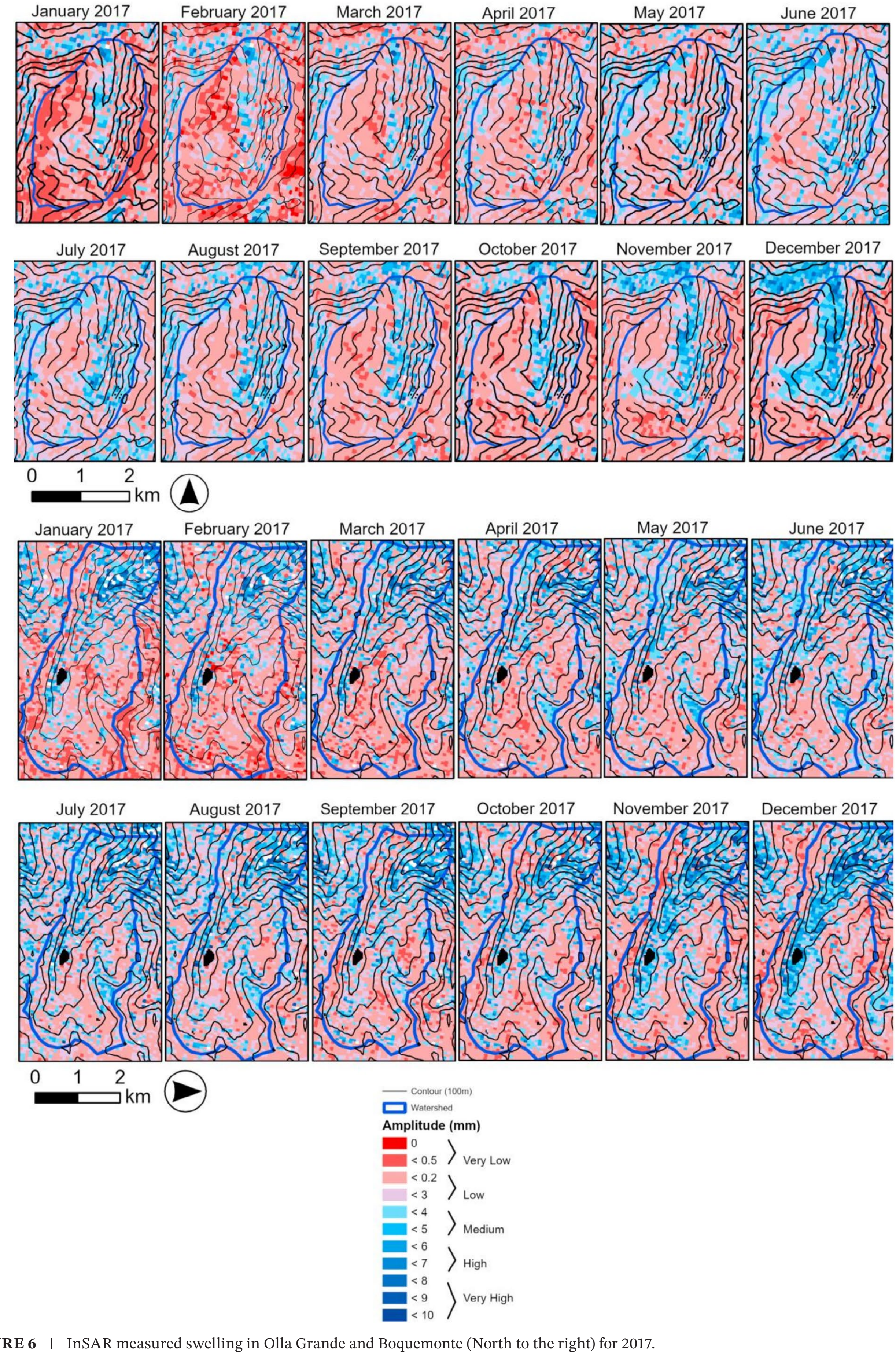

FIGURE 6 | InSAR measured swelling in Olla Grande and Boquemonte (North to the right) for 2017.

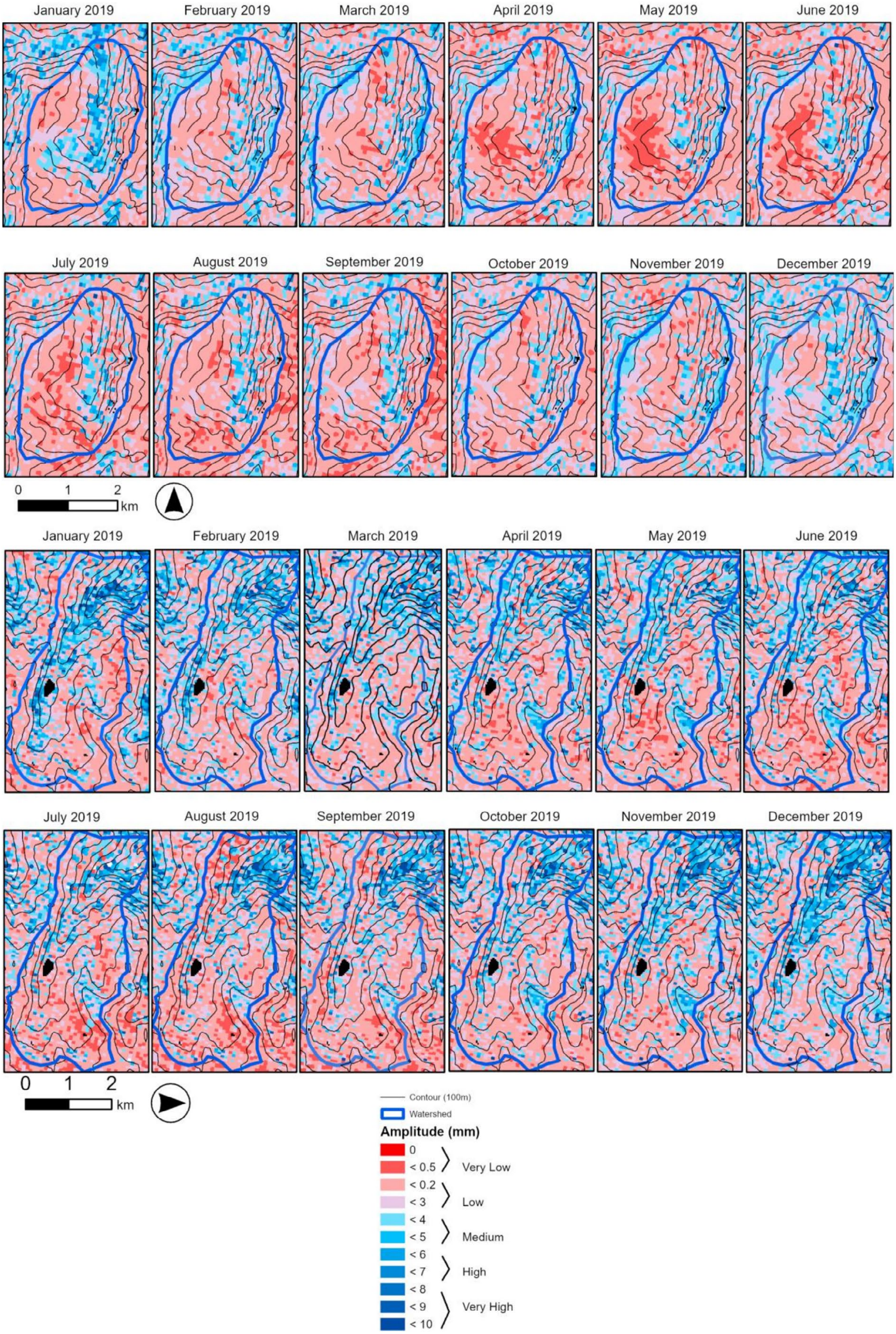

FIGURE 7 | InSAR measured swelling in Olla Grande and Boquemonte (North to the right) for 2019.

swelling feature in the valley similar to the starting point of January 2019.

4.1.2 | Boquemonte

Although a much more complex basin, Boquemonte displays an almost identical transition between the monthly swelling extremes to Olla Grande (Figures 6 and 7). For example, dry season high to very high swelling on the valley floor was flanked by medium and low swelling e.g., during December 2017 and January 2019. Accordingly, medium to high swelling is found on the ridges and low to medium swelling is found on the slopes during June 2017 and June 2019. The generally greater swelling observed on slopes with a western aspect in Olla Grande is less pronounced because this is a westward draining basin, but some evidence for this is observed on the western slopes of the small spurs that divide the various northerly sub-basins within Boquemonte. Of particular note is a feature that consistently develops into medium level swelling in the north eastern area of the site. In 2017 this area does not retain high levels of swelling when the second pulse of precipitation was weak, whereas at other times it appears capable of ponding and holding wet season precipitation longer than surrounding ridges and slopes. Google imagery indicates a depression in this ridge. Swelling is consistently high in the lower reaches of Boquemonte, but the magnitude is more uncertain as this is where it is more heavily forested than the lower reaches of Olla Grande.

4.1.3 | Páramo Guantiva-La Rusia

On a monthly time step, the simultaneous behaviour observed in the two drainage basins is present across the whole páramo. For brevity and detail, the wet season ridge and upper slope swelling and dry season valley swelling are shown for the central section of the Guantiva-La Rusia ridge (Figure 8). Of these two seasons, the maximum swelling of the broader valley floors is greater than the maximum swelling on the narrower ridges. For the same section, a land cover map depicting the main biomass categories and the multiannual velocity standard error shows where topography and biomass are more likely to combine to increase noise and uncertainty in the results (Figure 9). Areas of high uncertainty occur where time series have been interpolated over radar shadow across the line-of-sight in some mainly east-facing deep and steep-sided valleys. There is no overall bias with or across the satellite line-of-sight as the error map shows no evidence of mosaic-like segmentation corresponding to different cardinal slope aspects. As anticipated, the greater standard error has a strong relationship with land cover of greater biomass, and not the patterns of seasonal surface motion. Errors on the ridges and upper slopes are generally very low where there is low biomass páramo consisting of grassland and pasture vegetation cover. The standard error on the lower slopes in forest below the upper montane tree line and in the areas of intensive agriculture away from typical grassland and pasture páramo vegetation is high. Regardless of standard error, swelling can be traced up the valleys because in this tropical setting the leaf cover on the woody vegetation is more or less constant and does not seasonally influence the timing of surface motion, only the uncertainty in magnitude.

4.2 | Interpretation

To interpret these patterns of behaviour, we assume that swelling and shrinking of the land surface, recorded by InSAR, is a response to change in water storage within the soil or superficial deposits that dominates over vegetation growth and soil moisture effects on the InSAR signal (Westerhoff and Steyn-Ross 2020). We do not see low biomass vegetation growth quickly respond to precipitation in the valleys as the first valley swell is delayed, subdued and does not correspond to the onset of earlier precipitation and swelling on the ridges (Figure 5). The second dry season swell occurs when clearer skies, reduced precipitation and increased evapotranspiration dominate, so during this period low biomass vegetation growth is suppressed and coupled with a lack of seasonality of any higher biomass vegetation presence, soil swelling must dominate. The dominant driving force behind surface motion is either a change in one or both of effective stress and swelling on account of adsorption of water with clay or organic matter within the soil. Swelling is presumed to occur when the amount of water stored in soils or other superficial deposits within the area of a pixel increases, and shrinking occurs when the amount of water stored in the same deposits decreases in that pixel. Swelling is maintained when rates of water input by infiltration or lateral flow exceed rates of output by lateral flow or evapotranspiration, resulting in the soils or superficial deposits becoming more saturated closer to the surface. However, on the ridges, it is less easy to discriminate actual soil swelling from vegetation growth and soil moisture effects on the InSAR signal because rainwater is simultaneously feeding vegetation growth and filling soil pores. The influence of soil moisture on the InSAR signal may well be proportionally greater, but with a high organic content in these soils, physical swelling is most likely to remain dominant.

4.2.1 | Precipitation and Swelling

The most notable observation is that similar, spatially consistent patterns of swelling and shrinking behaviour happen simultaneously in the two study basins and regionally across the Guantiva-La Rusia range. In the wet season, there is marked swelling on the ridges and upper slopes, consistent with infiltration and increased saturation of ridge and slope soils in direct response to periods of greater precipitation. More pronounced swelling on ridges and upper slopes can be found on the leeward western aspects in comparison to windward eastern aspects, potentially a result of the influence of prevailing easterly winds on evapotranspiration on the exposed upper slopes. Swelling is least pronounced on the steeper mid-slopes where slope gradients may promote surface runoff and reduce water infiltration.

The most striking feature in the hydrological year is the marked swelling of the valley floors towards the end of the wet season and into the dry season (circ. December to February).

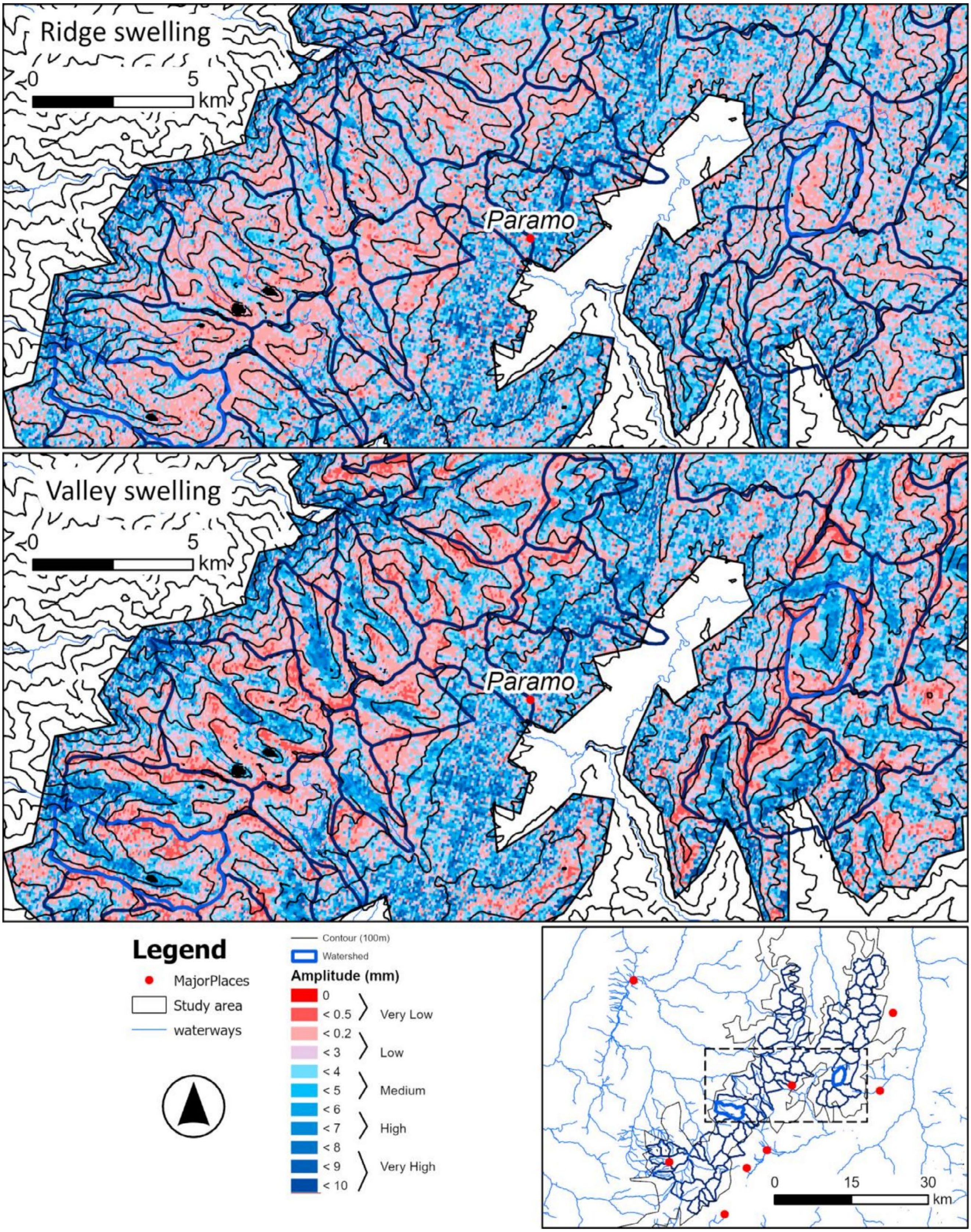

FIGURE 8 | Amplitude of swelling across the central portion of the study zone for wet June 2017 (upper panel), and dry February 2020 (middle, panel) seasons. Neighbouring drainage basins are plotted with Boquemonte and Olla Grande to highlight ridge and valley topography. Whilst the amplitudes are random around the fringes of the study area below the upper montane treeline, the greatest amplitudes of swelling are uniform over the ridges and greater than swelling over the steep valley sides in June 2017, and greater in the valleys and less on the slopes and ridges for a late dry season in February 2020. Plotting similarly sized drainage basins across the whole of the Guantiva-La Rusia páramo illustrates the regional extent of this swelling behaviour (lower panel), which may be applicable across all páramos in the Andes mountains.

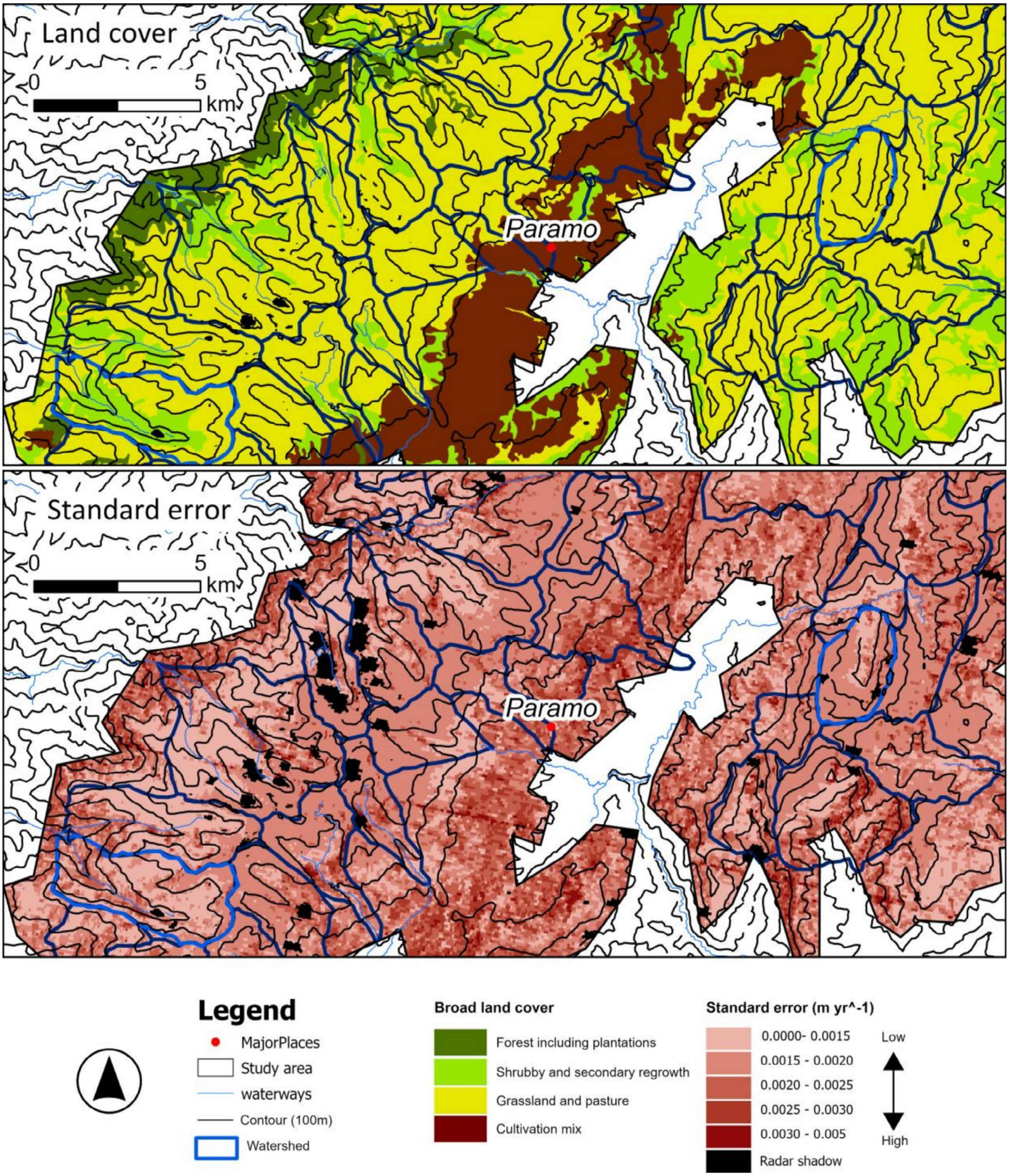

FIGURE 9 | Broad land cover classes (upper panel) and multiannual velocity standard error (lower panel) across the central portion of the study zone. Land cover classes are compiled into four groups of biomass: Forest, shrubby, grasslands, and pasture, and a cultivation mix from the land cover map of Colombia (IDEAM 2014). Standard error is in m year^{-1} (Cigna and Sowter 2017).

Additionally, throughout the year, localised lower magnitude swelling of the valley floor is present in the data. We found that this swelling is more extensive around August to September, which also corresponds to a period of seasonally reduced rainfall. The August to September swelling is not of the same magnitude as the swelling observed in December and February. In the complete time series (SM Figures S1 and S2), valley floor swelling appears to be larger and more extensive in years with overall higher total precipitation e.g., 2018/19 and 2019/20 and less in years with lower total precipitation e.g., 2016/17. In the valleys, surface motion from soil swelling must dominate over the effects of vegetation and soil moisture effects on the InSAR signal as high biomass shrubs and trees do not disperse seeds, colonise, establish, die back, and recede on these time scales, so the soil swelling must be fed by antecedent precipitation from the previous months. Swelling of the valley floor tends to concentrate in areas of confluence and dissipate downstream with swelling reducing first in the upper valley and lower slopes, and finally being concentrated towards the basin exit. This is consistent with expected drainage patterns.

The late wet season into dry season swelling does not always display a clear relationship to antecedent precipitation events in the preceding few months, for example, the swelling in November–December 2017 (Figure 6) followed a relatively dry second half of the 2017 wet season. Nor does the swelling of the valley floor build progressively through the year, for example, we found that the valley floor swelling was lowest in October 2018 just 2 months before marked swelling in December 2018 (SM Figure S2). Also, periods of intense precipitation earlier in the wet season, as inferred from the rainfall record and observed as swelling on upper slopes and ridge crests, do not lead to notable swelling on the valley floors and lower slopes. This may indicate the impact of antecedent moisture conditions, in which ridge and slope soils are re-wetting and retaining water early in the wet season with limited drainage.

4.2.2 | Valley Floor Swelling

Water flow and storage in upland páramo environments is considered to be in shallow flow systems where deeper infiltration and groundwater flows are negligible whilst the hydrological mechanisms of lower valley sediments are not yet well understood. Using this comprehension, during the main wet season, the first swelling in the valley bottoms is limited because the upslope and ridge soils are in a dryer empty state and release little water. The later swelling in the valley floors would follow because the ridge soils are wetted and forced to release water during the later smaller wet season, thus leading to a piston flow mechanism. The unusual timing and swelling observed on the lower valley floor may then be explained by field capacity of the upland soils and antecedent conditions driving the magnitude and timing of swelling. However, this mechanism works on the assumption that the composition of the lower valley sediment does not significantly influence flow and storage.

The patterns of swelling of the valley floors are consistent with a hypothesis of slower, somewhat deeper, cumulative storage of water within sediments in the valley floor during the wet to dry season transition. This swelling pattern then begins to diminish during the dry season. During the wet season, valley floor swelling, although present, is less extensive and of lower magnitude during months with high precipitation, indicating that much of this precipitation is rapidly lost through the system via overland flow or movement in the shallow subsurface. These results suggest that the extensive late wet to dry season transition valley floor swelling is most consistent with the slow accumulation of shallow groundwater during the wet season (Figure 10), and the lack of direct response to precipitation indicates that this storage probably represents a small proportion of total precipitation. That only a small proportion of the precipitation enters groundwater storage is consistent with the findings of others (Glas et al. 2019). It also suggests that somewhat deeper groundwater storage may help sustain rivers during the dry season (Glas et al. 2019; Karlsen et al. 2016).

Another possibility that could contribute to valley floor swelling is a result of a slow outgoing flux of stored water from valley wetlands and their connectivity to the river network (Wunderlich et al. 2023). Some of these wetlands may simply overflow straight away, while other wetlands may be disconnected from the river network and fill up as subsurface flow comes in, with storage extending into the dry season (Wunderlich et al. 2023). These mechanisms require a direct response of the wetlands to precipitation, so they do not explain the timing and the lack of progressive increase in valley floor swelling throughout the wet season. Nor do these mechanisms provide an explanation for the variable spatial extent of valley swelling, an observation that is more compatible with a spatially variable increase in the height of a shallow water table.

Slow steady accumulation of shallow groundwater from upslope initially appears at odds with the abrupt onset of swelling in the dry season. However, this may be a consequence of groundwater entering more elastic, less confined near-surface soils and sediments rather than any nonlinearity in the water accumulation process.

Although exact timings differ between years, that similar patterns of behaviour with identical timings are observed across the entire páramo Guantiva-La Rusia is probably a result of similar catchment size, climate, basin properties, and superficial geology across the region. The regional geomorphic development of this area has determined that basin properties and superficial deposits have evolved by similar patterns of uplift, glaciation, fluvial processes, and mass movement. In this context, it is notable that areas displaying consistent behaviour are generally within the maximum glacial extent expected in the Andes (Bryan and Helmens 2005) and therefore more likely to contain notable quantities of moraine, fluvio-glacial deposits, and colluvium.

5 | Discussion

Two notable results arise from this work, one related to the hydrological observations and the other related to the application of InSAR for the purpose of making hydrological observations in montane environments.

In terms of the hydrological observations, the InSAR results are consistent with the expected patterns of behaviour i.e., following precipitation soils will swell due to infiltration. The flow is rapid, lateral to the surface, and dominated by shallow hillslope flow. The flow occurs within a thin soil layer that has formed since the last glacial period (Ochoa-Tocachi et al. 2019). In addition to this, the InSAR results also provide evidence for a deeper slower process of shallow groundwater accumulation over the duration

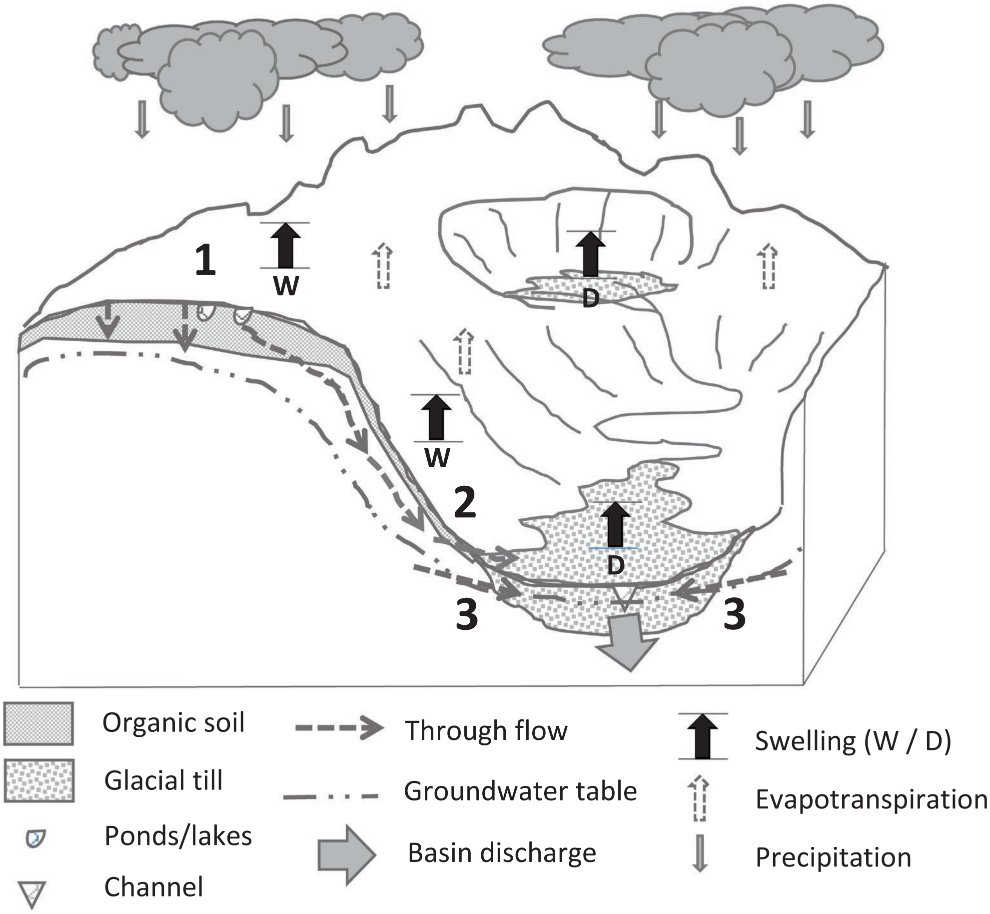

FIGURE 10 | Conceptualisation of the mechanisms of annual water storage and surface movement in the páramo, showing the subsurface materials, throughflow paths, core areas and season of maximum recharge, and transgression where interannual variation determines maximum recharge timing. (1) Ridge swelling from infiltration during the wet season. (2) Swelling further downslope as subsurface moisture progresses downslope through thin soils. (3) Deeper infiltration during the wet season rains has a longer slower flow path before feeding into glacial material much later in the dry season, or late in the wet season depending on antecedent conditions. Flow to the main valley may go directly to the valley floor or may drain into deposits in hanging valleys or moraine-like features on valley sides (not shown) before reaching the valley floor. W is the wet season, D is dry season.

of the hydrological year. This is consistent with deeper infiltration (Lazo et al. 2019), longer transit times (Lazo et al. 2019) and accumulation of groundwater in superficial deposits on valley floors (Glas et al. 2019; Karlsen et al. 2016). While initially appearing somewhat at odds with the observations of Ochoa-Tocachi et al. (2019), the discrepancies between these ideas can be resolved by re-considering the volumes of water in either pathway. If the majority of precipitation is rapidly lost and only a small share contributes to shallow groundwater, deeper slower accumulation of water is to be expected (Glas et al. 2019). This leads to the question as to whether shallow groundwater is significant in terms of hydrological resilience during the dry season or in sustaining bofedales (high altitude wetlands with organic rich peaty soils) which in turn enhance hydrological resilience.

The role of shallow ground water in helping to sustain rivers during the dry season can be tested by measurement, but that would need to take place in strategic parts of the basin. Many páramo studies tend to measure below the scale of basins defined in this study, concentrating on higher altitude sub-valleys often in the order of a few km^2 whilst rarely considering lower reaches. These smaller basins are too high in the watershed and too steep to enable our inferred groundwater influence on baseflow to be tested. However, retrospectively, if the InSAR observation is correct, measures of baseflow targeted in the right positions should show a corresponding late wet season–early dry season rise in discharge, and the absence of these field measures increases uncertainty in our conclusion. Measurements with parent catchments are rare and have been able to identify delayed flows in montane systems, albeit through deeper groundwater (Kosugi et al. 2011; Asano et al. 2020). Additionally, water chemistry could help confirm if delayed subsurface flow or a piston flow explains later swelling into the valleys. Water sampling at strategic depths and locations in the watersheds using isotope tracers and end-member analysis is a common approach, particularly in glaciated watersheds in order to segregate seasonal sources, age, and provenance (Baraer et al. 2015; Correa et al. 2017; Lazo et al. 2019; Cetina et al. 2020) but usually lacks sampling in the lower reaches. The absence of glacial meltwater in this environment may simplify the analysis and detect deep groundwater flows if present.

Another important contributor to basin resilience is bofedales, which are considered to rapidly recharge during the wet season and slowly discharge during the dry season (Ross et al. 2023).

Comparing the reported distribution of histosols (Figure 3) to areas of late wet season/dry season swelling indicates that these soils tend to be found in areas that display marked swelling. This association is consistent with observations from other páramo areas (Correa et al. 2017; Lazo et al. 2019; Cetina et al. 2020), in which peat and histosols (Figure 3) mainly occur in hanging valleys and valley floors where groundwater discharge can maintain soil saturation. This requirement for groundwater may explain the relative scarcity of peat soils within the páramo and their vulnerability to extreme hydrological seasonality (Cobb et al. 2017; Oyague et al. 2022), although these studies were limited to dryer or lowland regions. However, the subsurface flow feeding these wetlands has been observed to be shallow, relatively rapid flow that behaves like a linear reservoir, i.e., contribution is maximum just after a rainfall event (Ross et al. 2023). A possible resolution to the influence of groundwater and the reality of observed behaviour may revolve around the question of bofedal development in which groundwater seepage would enhance the probability of wet soils being sustained during the dry season with subsequent evolution of the bofedal system isolating them from the initiating influence of groundwater. It may also be that in periods of extreme hydrological stress groundwater seepage could still lend some resilience to bofedales.

The results and their interpretation indicate that InSAR measures of surface motion have the potential to provide data on the hydrological characteristics and behaviour of montane basins on a regional scale. Despite variations in soil type, vegetation, and geology, the InSAR measures illustrate systematic hydrological behaviour in the basins across a wide area. We therefore conclude these measures or data derived from them could be used to test and refine models of basin hydrology and to compare the hydrological characteristics of basins (Figure 10).

For example, surface motion could be used to map recharge and soil water storage characteristics (Guerrón-Orejuela et al. 2023) based on the timing and amplitude of swelling following rainfall, with high amplitude swelling indicating a high capacity for capturing and storing water and vice versa. Using this approach, basins can be compared and ranked based on their relative water storage and recharge characteristics, for example, the percentage of area displaying a high amplitude response to the first wet season. In turn, this could be used as a baseline measure of basin condition to quantify the impact of land management decisions, understand the impact of regional climate change on groundwater resources, and identify areas requiring regulatory protection. The systematic hydrological behaviours could also be used to better target field measurements.

The method has for the first time revealed monthly surface motion in this páramo landscape, usefully providing qualitative data that has challenged hydrological models and can strategically direct field research. We observe consistency, do not have a significant bias in motion patterns with satellite geometry and topography, and acknowledge increased uncertainty in forested, shrubby and agricultural areas. A limitation of the method is that it underestimates the true surface motion, and it must not be considered as an accurate measure of surface displacement. Interpretation is therefore dependent on the precision of the seasonal signal and all work to date indicates that this provides an accurate measure of direction of motion and a precise measure of relative magnitude, i.e., we can be confident that relative changes in amplitude are a true indicator of differences on the ground (Marshall et al. 2022). Validation and calibration from field data will improve quantification of surface motion towards absolute accuracy and enhance the application of the InSAR. As this is an intensive costly exercise (Marshall et al. 2022), the different levels of uncertainty indicate careful planning across multiple circumstances, such as biomass transitions and agricultural areas, at different scales is required. Another limitation is the frequency of the satellite acquisitions which means that we can only reliably observe processes operating on a time frame of a month or more.

An important advantage of the method is that it can provide near continuous data coverage over whole mountainous regions and multiple seasons regardless of climate, terrain, and sociopolitical pressures that may limit access. It can therefore enable rapid assessment and continuous monitoring of hydrological behaviour that would otherwise be impractical to do.

Acknowledgements

This work was supported by the Natural Environment Research Council, United Kingdom, project PARAGUAS, grant NE/R017654/1. Thanks to IDEAM—Instituto de Hidrología, Meteorología y Estudios Ambientales (Colombia) for open source meteorological data and weather station data from Estación Guantentá de Parques Nacionales Naturales-PNN, Colombia, application 20219050026612. Germán Eduardo Cely Reyes, Diego Fernando Monero Pérez of UPTC—Universidad Pedagógica y Tecnológica de Colombia, Tunja, Colombia, for advice and data support. Germán Grimaldos, Nicomedes Aparicio and Alvaro Álvarez for guiding us around the Guantiva-La Rusia páramo.

Data Availability Statement

Motion time series data can be obtained from the authors (or at Nottingham repository doi: 10.17639/nott.7550). Climate data can be found at Instituto de Hidrología, Meteorología y Estudios Ambientales, Tiempo y Clima. (IDEAM) http://www.ideam.gov.co/web/tiempo-y-clima/climatologico-mensual. Digital elevation data from the Shuttle Radar Topography Mission can be found at http://srtm.csi.cgiar.org. Shapefiles from the 'General soil study of the Instituto Geográfico Agustín Codazzi' Colombia, can be downloaded from the IGAC website, https://www.igac.gov.co/.

References

Aggarwal, A., H. Frey, G. McDowell, et al. 2022. "Adaptation to Climate Change Induced Water Stress in Major Glacierized Mountain Regions." *Climate and Development* 14, no. 7: 665–677. https://doi.org/10.1080/17565529.2021.1971059.

Alshammari, L., D. S. Boyd, A. Sowter, et al. 2020. "Use of Surface Motion Characteristics Determined by InSAR to Assess Peatland Condition." *Journal of Geophysical Research: Biogeosciences* 125: e2018JG004953. https://doi.org/10.1029/2018JG004953.

Asano, Y., M. Kawasaki, T. Saito, et al. 2020. "An Increase in Specific Discharge With Catchment Area Implies That Bedrock Infiltration Feeds Large Rather Than Small Mountain Headwater Streams." *Water Resources Research* 56: e2019WR025658. https://doi.org/10.1029/2019WR025658.

Baraer, M., J. McKenzie, B. G. Mark, et al. 2015. "Contribution of Groundwater to the Outflow From Ungauged Glacierized Catchments: A Multi-Site Study in the Tropical Cordillera Blanca, Peru." *Hydrological Processes* 29: 2561–2581. https://doi.org/10.1002/hyp.10386.

Bounous, M., T. Condom, R. I. Meneses, P. Vincent, C. Garcia, and F. Anthelme. 2018. "Cushion Plants and Herbivory Drive the Water-Holding Capacity of the High Andean Peatlands in Bolivia. Geophysical Research Abstracts, (20). EGU 2018–7160, 2018 EGU General Assembly." https://meetingorganizer.copernicus.org/EGU2018/EGU2018-7160.pdf.

Bradley, A. V., R. Andersen, C. Marshall, A. Sowter, and D. J. Large. 2022. "Identification of Typical Ecohydrological Behaviours Using InSAR Allows Landscape-Scale Mapping of Peatland Condition." *Earth Surface Dynamics* 10, no. 2: 261–277. https://doi.org/10.5194/esurf-10-261-2022.

Bradley, R. S., M. Vuille, H. F. Diaz, and W. Vergara. 2006. "Threats to Water Supplies in the Tropical Andes." *Science* 312, no. 5781: 1755–1756. https://doi.org/10.1126/science.1128087.

Brück, S. A., B. D. Torres, and M. Polizeli. 2023. "The Ecuadorian Paramo in Danger: What We Know and What Might Be Learned From Northern Wetlands." *Global Ecology and Conservation* 47: e02639. https://doi.org/10.1016/j.gecco.2023.e02639.

Bryan, G. M., and K. F. Helmens. 2005. "Reconstruction of Glacier Equilibrium-Line Altitudes for the Last Glacial Maximum on the High Plain of Bogotá, Eastern Cordillera, Colombia: Climatic and Topographic Implications." *Journal of Quaternary Science* 20, no. 7–8: 789–800. https://doi.org/10.1002/jqs.974.

Buytaert, W., R. Célleri, B. De Biévre, et al. 2006. "Human Impact on the Hydrology of the Andean Páramos." *Earth Science Reviews* 79, no. 1–2: 53–72. https://doi.org/10.1016/j.earscirev.2006.06.002.

Cárdenas, M. A., C. Tobón, and B. N. Rock. 2018. "Ecophysiology of Frailejones (*Espeletia* Spp.), and Its Contribution to the Hydrological Functioning of páramo Ecosystems." *Plant Ecology* 219: 185–198. https://doi.org/10.1007/s11258-017-0787-x.

Cetina, M., J.-D. Taupin, S. Gómez, and N. Patris. 2020. "Hydrodynamic Conceptual Model of Groundwater in the Headwater of the Rio de Oro, Santander (Colombia) by Geochemical and Isotope Tools." *Water Supply* 20, no. 4: 1567–1579. https://doi.org/10.2166/aqua.2020.114.

Cigna, F., and A. Sowter. 2017. "The Relationship Between Intermittent Coherence and Precision of ISBAS InSAR Ground Motion Velocities: Ers-1/2 Case Studies in the UK." *Remote Sensing Environment* 202: 177–198. https://doi.org/10.1016/j.rse.2017.05.016.

Cobb, A. R., A. M. Hoyt, L. Gandois, et al. 2017. "How Temporal Patterns in Rainfall Determine the Geomorphology and Carbon Fluxes of Tropical Peatlands." *Proceedings of the National Academy of Sciences of The United States of America* 114, no. 26: E5187–E5196. https://doi.org/10.1073/pnas.1701090114.

Comas, X., N. Terry, J. A. Hribljan, et al. 2017. "Estimating Below-Ground Carbon Stocks in Peatlands of the Ecuadorian Páramo Using Ground-Penetrating Radar (GPR)." *Journal of Geophysical Research, Biogeosciences* 122: 370–386. https://doi.org/10.1002/2016JG003550.

Correa, A., D. Windhorst, D. Tetzlaff, et al. 2017. "Temporal Dynamics Indominant Runoff Sources and Flowpaths in the Andean Paramo." *Water Resources Research* 53: 5998–6017. https://doi.org/10.1002/2016WR020187.

Crespo, P., R. Célleri, W. Buytaert, et al. 2009. "Land Use Change Impacts on the Hydrology of Wet Andean Páramo Ecosystems." In *Proceedings of Workshop, Status and Perspectives of Hydrology in Small Basins*, vol. 336, 2010. IAHS Publ. https://doi.org/10.13140/2.1.5137.6320.

Earle, L. R., B. G. Warner, and R. Aravena. 2003. "Rapid Development of an Unusual Peat-Accumulating Ecosystem in the Chilean Altiplano." *Quaternary Research* 59: 2–11. https://doi.org/10.1016/S0033-5894(02)00011-X.

ESRI. 2024. "World View Source: Esri, Maxar, Earthstar Geographics, and the GIS User Community."

Farr, T. G., P. A. Rosen, E. Caro, et al. 2007. "The Shuttle Radar Topography Mission." *Reviews of Geophysics* 45, no. 2: 1–33. https://doi.org/10.1029/2005RG000183.

Giles, M. P., N. Michelutti, C. Grooms, and J. P. Smol. 2017. "Long-Term Limnological Changes in the Ecuadorian Páramo: Comparing the Ecological Responses to Climate Warming of Shallow Waterbodies Versus Deep Lakes." *Freshwater Biology* 63: 1316–1325. https://doi.org/10.1111/fwb.13159.

Glas, R., L. Lautz, J. McKenzie, et al. 2019. "Hydrogeology of an Alpine Talus Aquifer: Cordillera Blanca, Peru." *Hydrogeology Journal* 27, no. 6: 2137–2154. https://doi.org/10.1007/s10040-019-01982-5.

Guerrón-Orejuela, E. J., K. C. Rains, T. M. Brigino, et al. 2023. "Mapping Groundwater Recharge Potential in High Latitude Landscapes Using Public Data, Remote Sensing, and Analytic Hierarchy Process." *Remote Sensing* 15, no. 10: 2630. https://doi.org/10.3390/rs15102630.

Hrysiewicz, A., E. P. Holohan, S. Donohue, and H. Cushnan. 2023. "SAR and InSAR Data Linked to Soil Moisture Changes on a Temperate Raised Peatland Subjected to a Wildfire." *Remote Sensing of Environment* 291: 113516. https://doi.org/10.1016/j.rse.2023.113516.

IDEAM. 2014. "Shapefiles From 'Cobertura de la Tierra Metodología CORINE Land Cover Adaptada Para Colombia Durante el Periodo 2010-2012, 1:100.000'. Instituto de Hidrología, Meteorología y Estudios Ambientales, Tiempo y Clima, República de Colombia." http://www.ideam.gov.co/.

IDEAM. 2022. "Instituto de Hidrología, Meteorología y Estudios Ambientales, Tiempo y Clima." http://www.ideam.gov.co/web/tiempo-y-clima/climatologico-mensual.

IGAC. 2005. "Shapefiles From the 'General Soil Study of the Instituto Geográfico Agustín Codazzi', Colombia." https://www.igac.gov.co/.

Islam, M. T., A. V. Bradley, A. Sowter, et al. 2022. "Potential Use of APSIS-InSAR Measures of the Range of Vertical Surface Motion to Improve Hazard Assessment of Peat Landslide." *Mires and Peat* 28: 21. https://doi.org/10.19189/MaP.2021.OMB.StA.2356.

Jarvis, A., H. I. Reuter, A. Nelson, and E. Guevara. 2008. "Hole-Filled Seamless SRTM Data V4, International Centre for Tropical Agriculture (CIAT)." http://srtm.csi.cgiar.org.

Kang, S., and R. Knight. 2023. "Isolating the Poroelastic Response of the Groundwater System in InSAR Data From the Central Valley of California." *Geophysical Research Letters* 50, no. 9: e2023GL103222. https://doi.org/10.1029/2023GL103222.

Karlsen, R. H., T. Grabs, K. Bishop, I. Buffam, H. Laudon, and J. Seibert. 2016. "Landscape Controls on Spatiotemporal Discharge Variability in a Boreal Catchment." *Water Resources Research* 52, no. 8: 6541–6556. https://doi.org/10.1002/2016WR019186.

Kosugi, K., M. Fujimoto, S. Katsura, H. Kato, Y. Sando, and T. Mizuyama. 2011. "Localized Bedrock Aquifer Distribution Explains Discharge From a Headwater Catchment." *Water Resources Research* 47, no. 7: W07530. https://doi.org/10.1029/2010WR009884.

Large, D. J., A. V. Bradley, E. Mitchell, C. Fallaize, I. Dryden, and R. Andersen. 2025. "Application of Surface Motion Remote Sensing to Quantify the Condition and Trajectory of Change of c.680,000 ha of Peatland." *NatureScot Research Report*: 1356. https://www.nature.scot/doc/naturescot-research-report-1356-application-surface-motion-remote-sensing-quantify-condition-and.

Lazo, P. X., G. M. Mosquera, J. J. McDonnell, and P. Crespo. 2019. "The Role of Vegetation, Soils, and Precipitation on Water Storage and Hydrological Services in Andean Páramo Catchments." *Journal of Hydrology* 572: 805–819. https://doi.org/10.1016/j.jhydrol.2019.03.050.

Maldonado Fonkén, M. S. 2014. "An Introduction to the Bofedales of the Peruvian High Andes." *Mires and Peat* 15: 5. http://www.mires-and-peat.net/pages/volumes/map15/map1505.php.

Marshall, C., H. P. Sterk, P. J. Gilbert, et al. 2022. "Multiscale Variability and the Comparison of Ground and Satellite Radar Based Measures of Peatland Surface Motion for Peatland Monitoring." *Remote Sensing* 14, no. 2: 336. https://doi.org/10.3390/rs14020336.

Mills-Novoa, M., S. L. Borgias, A. Crootof, B. Thapa, R. de Grenade, and C. A. Scott. 2017. "Bringing the Hydrosocial Cycle Into Climate Change Adaptation Planning: Lessons From Two Andean Mountain Water Towers." *Annals of the American Association of Geographers* 107, no. 2: 393–402. https://doi.org/10.1080/24694452.2016.1232618.

Mitchell, E. G., I. L. Dryden, C. J. Fallaize, et al. 2024. "Object Oriented Data Analysis of Surface Motion Time Series in Peatland Landscapes." *Journal of the Royal Statistical Society: Series C: Applied Statistics* 74, no. 2: 406–428. https://doi.org/10.1093/jrsssc/qlae060.

Mitchell, E., C. Fallaize, I. Dryden, A. V. Bradley, D. J. Large, and R. Andersen. 2025. "A Summary of Surface Motion Remote Sensing." *NatureScot Research Report*: 1355. https://www.nature.scot/doc/naturescot-research-report-1355-summary-surface-motion-remote-sensing-methods-monitoring-peatland#change-detection.

Moreau, S., R. Bosseno, X. F. Gu, and F. Baret. 2003. "Assessing the Biomass Dynamics of Andean Bofedal and Totora High-Protein Wetland Grasses From NOAA/AVHRR." *Remote Sensing of Environment* 85, no. 4: 516–529. https://doi.org/10.1016/S0034-4257(03)00053-1.

Mosquera, G. M., R. Hofstede, L. L. Bremer, et al. 2023. "Frontiers in Páramo Water Resources Research: A Multidisciplinary Assessment." *Science of the Total Environment* 892: 164373. https://doi.org/10.1016/j.scitotenv.2023.164373.

Ochoa-Tocachi, B. F., J. D. Bardales, J. Antiporta, et al. 2019. "Potential Contributions of Pre-Inca Infiltration Infrastructure to Andean Water Security." *Nature Sustainability* 2: 584–593. https://doi.org/10.1038/s41893-019-0307-1.

Ochoa-Tocachi, B. F., W. Buytaert, B. De Bièvre, et al. 2016. "Impacts of Land Use on the Hydrological Response of Tropical Andean Catchments." *Hydrological Processes* 30, no. 22: 4074–4089. https://doi.org/10.1002/hyp.10980.

Oyague, E., D. J. Cooper, and E. Ingol. 2022. "Effects of Land Use on the Hydrologic Regime, Vegetation, and Hydraulic Conductivity of Peatlands in the Central Peruvian Andes." *Journal of Hydrology* 609: 127687. https://doi.org/10.1016/j.jhydrol.2022.127687.

Peyre, G., D. Osorio, R. François, and F. Anthelme. 2021. "Mapping the Páramo Land-Cover in the Northern Andes." *International Journal of Remote Sensing* 42, no. 20: 7777–7797. https://doi.org/10.1080/01431161.2021.1964709.

Roa-García, M. C., S. Brown, H. Schreier, and L. M. Lavkulich. 2011. "The Role of Land Use and Soils in Regulating Water Flow in Small Headwater Catchments of the Andes." *Water Resources Research* 47, no. 5: W05510. https://doi.org/10.1029/2010WR009582.

Robledo, A. J., and B. C. Córdoba. 2000. "Distribución de La Precipitation en Colombia Analizada Mediante Conglomeración Estadística." *Cenicafé* 51, no. 2: 102–113. https://www.scribd.com/document/634172738/Untitled.

Ross, A. C., M. M. Mendoza, F. Drenkhan, et al. 2023. "Seasonal Water Storage and Release Dynamics of Bofedal Wetlands in the Central Andes." *Hydrological Processes* 37, no. 8: e14940. https://doi.org/10.1002/hyp.14940.

Schneider, W. 2024. "OpenStreetMap.org." https://extract.bbbike.org/.

Sheffield, J., E. F. Wood, M. Pan, et al. 2018. "Satellite Remote Sensing for Water Resources Management: Potential for Supporting Sustainable Development in Data-Poor Regions." *Water Resources Research* 54, no. 12: 9724–9758. https://doi.org/10.1029/2017WR022437.

Sidle, R. C. 2021. "Strategies for Smarter Catchment Hydrology Models: Incorporating Scaling and Better Process Representation." *Geoscience Letters* 8: 24. https://doi.org/10.1186/s40562-021-00193-9.

Smith, R. G., R. Knight, J. Chen, et al. 2017. "Estimating the Permanent Loss of Groundwater Storage in the Southern San Joaquin Valley, California." *Water Resources Research* 53, no. 3: 2133–2148. https://doi.org/10.1002/2016WR019861.

Smith, R., and R. Knight. 2019. "Modeling Land Subsidence Using InSAR and Airborne Electromagnetic Data." *Water Resources Research* 55, no. 4: 2801–2819. https://doi.org/10.1029/2018WR024185.

Somers, L. D., and J. M. McKenzie. 2020. "A Review of Groundwater in High Mountain Environments." *WIREs Water* 7, no. 6: e1475. https://doi.org/10.1002/wat2.1475.

Sowter, A., M. B. C. Amat, F. Cigna, S. Marsh, A. Athab, and L. Alshammari. 2016. "Mexico City Land Subsidence in 2014-2015 With Sentinel-1 IW TOPS: Results Using the Intermittent SBAS (ISBAS) Technique." *International Journal of Applied Earth Observation and Geoinformation* 52: 230–242. https://doi.org/10.1016/j.jag.2016.06.015.

Sowter, A., L. Bateson, P. Strange, K. Ambrose, and M. F. Syafiudin. 2013. "DInSAR Estimation of Land Motion Using Intermittent Coherence With Application to the South Derbyshire and Leicestershire Coalfields." *Remote Sensing Letters* 4, no. 10: 979–987. https://doi.org/10.1080/2150704X.2013.823673.

Squeo, F. A., B. G. Warner, R. Aravena, and D. Espinoza. 2006. "Bofedales: High Altitude Peatlands of the Central Andes Bofedales: Turberas de Alta Montaña de Los Andes Centrales." *Revista Chilena de Historia Natural* 79, no. 2: 245–255. https://doi.org/10.4067/S0716-078X2006000200010.

Tampuu, T., J. Praks, R. Uiboupin, and A. Kull. 2020. "Long Term Interferometric Temporal Coherence and DInSAR Phase in Northern Peatlands." *Remote Sensing* 12, no. 10: 1566–1588. https://doi.org/10.3390/rs12101566.

Toca, L., K. Morrison, R. R. E. Artz, A. Gimona, and T. Quaife. 2022. "High Resolution C-Band SAR Backscatter Response to Peatland Water Table Depth and Soil Moisture: A Laboratory Experiment." *International Journal of Remote Sensing* 43, no. 14: 5231–5251. https://doi.org/10.1080/01431161.2022.2131478.

Valois, R., N. Schaffer, R. Figueroa, et al. 2020. "Characterizing the Water Storage Capacity and Hydrological Role of Mountain Peatlands in the Arid Andes of North-Central Chile." *Watermark* 12, no. 4: 1071. https://doi.org/10.3390/w12041071.

Westerhoff, R., and M. Steyn-Ross. 2020. "Explanation of InSAR Phase Disturbances by Seasonal Characteristics of Soil and Vegetation." *Remote Sensing* 12, no. 18: 3029. https://doi.org/10.3390/rs12183029.

Wunderlich, W., M. Lang, K. Keating, W. B. Perez, and J. Oshun. 2023. "The Role of Peat-Forming Bofedales in Sustaining Baseflow in the Humid Puna." *Journal of Hydrology: Regional Studies* 47: 101394. https://doi.org/10.1016/j.ejrh.2023.101394.

Supporting Information

Additional supporting information can be found online in the Supporting Information section.